Atmos. Chem. Phys. Discuss., https://doi.org/10.5194/acp-2017-738
Manuscript under review for journal Atmos. Chem. Phys.
Discussion started: 10 November 2017

Atmospheric Chemistry and Physics Discussions

Technical Note: Evaluation of simultaneous measurements of mesospheric OH, HO_2, and O_3 under photochemical equilibrium assumption: Statistical approach

Mikhail Yu. Kulikov[1], Anton A. Nechaev[1], Mikhail V. Belikovich[1], Tatiana S. Ermakova[1], and Alexander M. Feigin[1]

[1]Institute of Applied Physics of the Russian Academy of Sciences, 46 Ulyanov Str., 603950 Nizhny Novgorod, Russia

Correspondence to: Mikhail Yu. Kulikov (mikhail_kulikov@mail.ru)

Abstract

The Technical Note presents a statistically correct approach to evaluating simultaneous measurements of several atmospheric components under the assumption of photochemical equilibrium. We consider simultaneous measurements of OH, HO_2, and O_3 at the altitudes of the mesosphere as a specific example and their daytime photochemical equilibrium as an evaluating relationship. A simplified algebraic equation relating local concentrations of these components in the 50-100 km altitude range has been derived. The parameters of the equation are air temperature, air concentration, local zenith angle, and the rates of 9 reactions. We have performed one-year simulation of the mesosphere and lower thermosphere using a 3D chemical-transport model. The simulation shows that the discrepancy between the calculated evolution of the components and the equilibrium value given by the equation does not exceed 3-4% in the full range of altitudes independent of season or latitude. We have developed the technique of statistic Bayesian evaluation of simultaneous measurements of OH, HO_2 and O_3 based on the equilibrium equation taking into account the measurement error. The first results of application of the technique to MLS/Aura data are presented in this Technical Note. It has been found that the satellite data of HO_2 distribution regularly demonstrates essentially lower altitudes of mesospheric maximum of this component. This has also been confirmed by offline retrieval of HO_2 from the MLS primary data.

Atmos. Chem. Phys. Discuss., https://doi.org/10.5194/acp-2017-738
Manuscript under review for journal Atmos. Chem. Phys.
Discussion started: 10 November 2017

Atmospheric Chemistry and Physics Discussions

1. Introduction

A prominent feature of the atmospheric photochemical systems is the presence of a large number of chemical components with short lifetime and concentrations close to stable photochemical equilibrium at every instant. The condition of balance between their sources and sinks is described by a system of algebraic equations. This system can be used to determine characteristics of hard to measure atmospheric species through other measurable components, validate results of remote or *in situ* measurements, estimate reaction rates usually known with significant uncertainty, and to understand processes and chemical reactions that influence variability of the most important atmospheric components, e.g. ozone, in the geographical region of interest.

This approach has found wide application:

(1) in 3D chemical transport models that include a large set of physical and chemical processes with a broad spectrum of spatio-temporal scales. In particular, the chemical family concept is widely used for simulating gas phase photochemistry of the lower and middle atmosphere (e.g., Douglass et al., 1989; Kaye and Rood, 1989; Rasch et al., 1995), when transport is taken into account only for the concentration of a chemical family, while relative concentrations of the constituent fast components are calculated from the instantaneous stable equilibrium condition. Complemented with the Henry law (e.g., Djouad et al., 2003; Tulet et al., 2006) in multiphase models, this approach markedly saves calculation time and increases the overall stability of the numerical scheme. Moreover, the use of the photochemical equilibrium condition to simulate fast components dynamics reduces the phase space dimension of box models significantly (e.g., Kulikov and Feigin, 2014), allowing a comprehensive analysis of nontrivial nonlinear dynamic properties of various atmospheric photochemical systems (e.g., Feigin and Konovalov, 1996; Feigin et al., 1998; Konovalov et al., 1999; Konovalov and Feigin, 2000; Kulikov et al., 2012).

(2) in investigations of the chemistry of the surface layer and free troposphere in different regions (over megalopolises, in rural areas, in the mountains, over the seas) based on measurements of nitrogen species, peroxy radicals, ozone, aerosols, and other components aimed at understanding processes impacting the surface ozone formation and air quality. The equilibrium condition is most frequently used for nitrogen species. For example, Chameides (1975) proposed a model for determining the vertical distribution of odd nitrogen, in which the HNO_3 profile could be

deployed to retrieve profiles of five other components (NO, NO_2, NO_3, N_2O_5, and HNO_2) from their photochemical equilibrium condition. In the paper by Stedman et al. (1975) the equation for NO_2 equilibrium that accounted only for the main source and sink of this component was applied to determine the photodissociation constant J(NO_2). A more accurate equation for the NO_2 equilibrium was used by Crawford et al. (1996) and Kondo et al. (1996) to determine the NO_2/NO partitioning and NO_x, allowing, in particular, investigating the spatial distribution of NO_x/NO_y over the Pacific.

Night-time equilibrium in the NO_2-NO_3-N_2O_5 system is used to determine surface layer N_2O_5 concentration, equilibrium constant of this system, equilibrium partitioning between NO_3 and N_2O_5, and loss coefficients of NO_3, N_2O_5 and NO_x (Martinez et al., 2000; Brown et al., 2003; Crowley et al., 2010; McLaren et al., 2010; Benton et al., 2010; Sobanski et al., 2016).

Platt et al. (1979) used the CH_2O photochemical equilibrium condition to analyse results of simultaneous measurement of CH_2O, O_3 and NO_2 and to identify mechanisms of CH_2O formation over rural areas and in maritime air. In the papers by Ko et al. (2003), Cantrell et al. (2003), Penkett et al. (1997), Penkett et al. (1998) algebraic expressions derived from equilibrium conditions for H_2O_2, peroxy radicals and nitrogen species were used to determine equilibrium values of peroxide concentration, total peroxy radical level, and NO/NO_2 ratio, and to diagnose the ozone production and loss levels in clean or polluted troposphere.

(3) in stratospheric chemistry studies, including determination of a critical parameter in catalytic cycles of ozone destruction in the polar stratosphere. In particular, the equilibrium condition for ClO and Cl_2O_2 along with the measurement data of daytime and night-time concentrations of these components in the polar stratosphere are used to evaluate the temperature dependence of the ClO concentration, reaction constants determining the $ClO + ClO + M \leftrightarrow Cl_2O_2 + M$ equilibrium, and the photolysis rate of Cl_2O_2 (Ghosh et al., 1997; Avallone et al., 2001, Solomon et al., 2002; Stimpfle et al., 2004; von Hobe et al., 2005; Berthet et al., 2005; Butz et al., 2007; von Hobe et al., 2007; Kremser et al., 2011; Sumińska-Ebersoldt et al., 2012; Wetzel et al., 2012).

Pyle et al. (1983) proposed a method for derivation of the OH concentration from satellite infrared measurements of NO_2 and HNO_3 using a simple algebraic relation following from the equilibrium condition for HNO_3. Algorithms for retrieving distributions of OH and HO2 from the satellite measurement data of O_3, NO_2, H_2O, HNO_3 by LIMS/Nimbus 7 and UARS with the help of algebraic models following from the photochemical equilibrium of O_x, HO_x and HNO_3 components

were proposed by Pyle and Zavody (1985), Pickett and Peterson (1996). It is also worthy of note that similar models are widely used for calculating concentrations of components with a short lifetime (e.g. $O(^1D)$ and OH) and subsequent evaluating vertical distributions of eddy diffusivity from measurements of trace gas concentration profiles (see, e.g., Massie and Hunten, 1981).

Kondo et al. (1988) made use of the photochemical equilibrium between NO and NO_2 for understanding diurnal variations of NO concentration measured during aircraft flights. In the paper by Webster et al. (1990) simultaneous *in situ* balloon-borne measurements of NO, NO_2, HNO_3, O_3 and N_2O and the photochemical equilibrium condition for various nitrogen components were used to determine OH, N_2O_5 and NO_y concentrations. A similar approach was employed by Kawa et al. (1990), who obtained NO_2, N_2O_5, $ClNO_3$, HNO_3 and OH concentrations from aircraft measurements of NO, ClO and O_3 concentrations. Hauchecorne et al. (2010) found that NO_3 concentration measured by GOMOS/ENVISAT positively correlates with temperature at altitudes up to 45 km in the region where NO_3 is in chemical equilibrium with O_3. Funke et al. (2005) used NO and NO_2 stable-state photochemistry to verify correctness of the new approach of retrieving distributions of those component from MIPAS/ENVISAT measurement data. Marchland et al. (2007) proposed a method to retrieve the temperature distribution in the stratosphere between 30 km and 40 km from O_3 and NO_3 measurements by GOMOS with the help of a simple equation derived from the night-time NO_3 chemical equilibrium.

(4) in investigations of the chemistry of O_x–HO_x components and atmospheric glows in the mesosphere and MLT area. In particular, Kulikov et al. (2006, 2009) proposed algorithms for the simultaneous retrieval of O, H, HO_2 and H_2O from joint OH and O_3 satellite measurement, in which the assumption of photochemical equilibrium of O_3, OH, and HO_2 was utilized. For several decades the assumption of the photochemical equilibrium of ozone (PEO) was widely used to determine distributions of atomic oxygen and atomic hydrogen at altitudes of the MLT via satellite and rocket measurement of ozone concentration and airglow emissions (e.g., Evans and Llewellyn, 1973; Good, 1976; Pendleton et al., 1983; McDade et al., 1985; McDade and Llewellyn, 1988; Evans et al., 1988; Thomas, 1990; Llewellyn et al., 1993; Llewellyn and McDade, 1996; Mlynczak et al., 2007, 2013a, 2013b, 2014; Smith et al., 2010; Siskind et al., 2008, 2015). Russell and Lowe (2003) applied PEO to infer the seasonal and global climatology of atomic oxygen using WINDII/UARS. PEO was deployed to investigate hydroxyl emission mechanisms, morphology, and variability in the upper mesosphere – lower thermosphere region (Marsh et al., 2006; Xu et al., 2010, 2012;

Kowalewski et al., 2014). Mlynczak and Solomon (1991, 1993) and Mlynczak et al. (2013b) used the equilibrium assumption to derive exothermic chemical heat. The PEO assumption employed for studying the mesospheric OH* layer response to gravity waves (Swenson and Gardner, 1998). In ultimately theoretical works, e.g. Grygalashvyly et al. (2014), Grygalashvyly (2015), PEO was used to derive the dependence of excited hydroxyl layer concentration and altitude on atomic oxygen and temperature. In the paper by Sonnemann et al. (2015) it was used to analyze annual variations of OH* layer. Moreover, PEO is frequently applied implicitly, when authors are equating the night-time loss of ozone in the reaction with atomic hydrogen and production of ozone by a 3-body reaction of molecular and atomic oxygen (e.g., Nikoukar et al., 2007).

In the present Technical note we demonstrate how the photochemical equilibrium condition of several atmospheric components may be employed to statistically correctly validate data of their simultaneous measurements, particularly in the case when measurement error is large.

We consider the simultaneous photochemical daytime equilibrium of OH, HO_2, and O_3 at the altitudes of the mesosphere. We have derived a simplified algebraic equation

$$F(OH, HO_2, O_3) = 1,$$

describing the relationship between local concentrations of the components at the altitudes of 50–100 km. The only parameters of the equation are air temperature, air concentration, local zenith angle, and constants of 9 reactions. One-year simulation of the mesosphere and lower thermosphere based on a 3D chemical-transport model shows that the discrepancy between the calculated evolution of the components and the equilibrium value given by the equation does not exceed 3–4 % in the full range of altitudes independent of season or latitude.

We have developed a technique of statistical Bayesian evaluation of simultaneous measurement of OH, HO_2 and O_3 based on the mentioned equilibrium equation taking into account the measurement error. The first results of its application to MLS/Aura data (Wang et al., 2015a,b; Schwartz et al., 2015) are presented. It is found that the satellite data of HO_2 distribution regularly demonstrates essentially lower altitudes of this component's mesospheric maximum. These results confirm the ones obtained via the offline retrieval of HO_2 from the MLS primary data (Millán et al., 2015).

The Technical Note is structured as follows. A 3D chemical transport model is briefly described in Sect. 2. In Sect. 3 a simplified algebraic relationship between the equilibrium concentrations of OH, HO_2 and O_3 is derived and verified by 3D simulations. Section 4 presents the

155 method of statistical evaluation of simultaneous data of OH, HO_2 and O_3. The results of applying
156 the method to MLS/Aura data are presented in Sect. 5. The last Section contains discussion of the
157 results followed by concluding remarks.
158
159 **2. Model and calculations**
160
161 For our calculations we used the global 3D chemical transport model (CTM) of the middle
162 atmosphere developed by the Leibniz Institute of Atmospheric Physics (IAP). It was designed
163 particularly for investigation of the spatio-temporal structure of phenomena in the MLT region and
164 specifically in the extended mesopause region. The model includes 3D advective and vertical
165 diffusive transport (turbulent and molecular). The grid-point model extends from the ground up to
166 the lower thermosphere (0–150 km; 118 pressure-height levels). The horizontal resolution amounts
167 to 5.625° latitudinally and 5.625° longitudinally. The chemistry module consists of 19 constituents,
168 49 chemical reactions, and 14 photo-dissociation reactions. CTM was described in numerous
169 papers (e.g., Sonnemann et al., 1998; Körner and Sonnemann, 2001; Grygalashvyly et al., 2009,
170 2011, 2012). It was validated, particularly for ozone, with measurement in a number of papers
171 (Hartogh et al., 2004, 2011; Sonnemann et al., 2006a, 2006b, 2007). Three-dimensional fields of
172 temperature and winds are used from the Canadian Middle Atmosphere Model (CMAM) for the
173 year 2000 (de Grandpre et al., 2000; Scinocca et al., 2008).
174 We calculated the annual variation of spatio-temporal distributions of OH, HO_2, and O_3 and
175 constructed distributions of the $F(OH, HO_2, O_3)$ function introduced in Sect. 1. To remove
176 transitional regions that correspond to sunset and sunrise, we took into account only periods of
177 local time with the solar zenith angle $\chi < 85°$. The previous research based on satellite
178 measurements had often showed results on pressure heights, or “pseudo altitudes”. Following
179 them, in the present paper we present our results on the pressure heights $z^* = -H\,ln(p / p_0)$,
180 where H = 7 km is the scale height, p is the pressure, and p_0 = 1013 hPa is the pressure at the
181 surface.
182
183 **3. Daytime photochemical equilibrium of OH, HO_2, and O_3 at the altitudes of the mesosphere**
184

Atmos. Chem. Phys. Discuss., https://doi.org/10.5194/acp-2017-738
Manuscript under review for journal Atmos. Chem. Phys.
Discussion started: 10 November 2017

Atmospheric Chemistry and Physics Discussions

The daytime balance of OH, HO_2, and O_3 concentrations at mesospheric altitudes is determined by the following primary reactions:

$O(^3P) + O_2 + M \rightarrow O_3 + M$, | k_1 (1)

$O_3 + h\nu \rightarrow O_2 + O(^1D, {}^3P)$, | $k_2 = J_{O3} = J_1 + J_2$ (2)

$O_3 + H \rightarrow O_2 + OH$, | k_3 (3)

$O + OH \rightarrow O_2 + H$, | k_4 (4)

$O + HO_2 \rightarrow O_2 + OH$, | k_5 (5)

$O_2 + H + M \rightarrow HO_2 + M$, | k_6 (6)

$O_3 + OH \rightarrow O_2 + HO_2$, | k_7 (7)

$H + HO_2 \rightarrow 2OH$ | k_8 (8)

$OH + HO_2 \rightarrow H_2O + O_2$ | k_9 (9)

where k_1–k_9 are the corresponding reaction constants, J_{O3} is the total dissociation rate of ozone, which is the sum of two branches, J_1 and J_2, and M is air concentration. Expressions for local concentrations of OH, HO2, and O_3 in the photochemical equilibrium are written in the form

$$OH = \left(k_3 \cdot O_3 \cdot H + k_5 \cdot HO_2 \cdot O + 2k_8 \cdot HO_2 \cdot H\right) / \left(k_4 \cdot O + k_7 \cdot O_3 + k_9 \cdot HO_2\right) \quad (10)$$

$$HO_2 = \left(k_6 \cdot M \cdot O_2 \cdot H + k_7 \cdot O_3 \cdot OH\right) / \left(k_5 \cdot O + k_8 \cdot H + k_9 \cdot OH\right) \quad (11)$$

$$O_3 = \frac{k_1 \cdot M \cdot O_2 \cdot O}{k_2 + k_3 \cdot H + k_7 \cdot OH} \quad (12)$$

Almost everywhere in the mesosphere and lower thermosphere (with the exception of 85-95 km, see Kulikov et al., 2017) the photodissociation reaction Eq. (2) is the main ozone sink, i.e. $k_2 >> k_3 \cdot H + k_7 \cdot OH$. Therefore, in the zero order approximation Eq. (12) can be simplified and the concentration of atomic oxygen can be defined in terms of ozone concentration:

$$O = \frac{k_2 \cdot O_3}{k_1 \cdot M \cdot O_2} \quad (13)$$

Making use of Eq. (13) we can derive from Eq. (11) an expression for the concentration of H in terms of concentrations of HO_2 and O_3. By substituting this equation and Eq. (13) into Eq. (10) we obtain an expression relating OH, HO_2, and O_3:

$$F(OH, HO_2, O_3) = \alpha \cdot \frac{k_4 \cdot OH}{k_5 \cdot HO_2} = 1, \quad (14)$$

where

Atmos. Chem. Phys. Discuss., https://doi.org/10.5194/acp-2017-738
Manuscript under review for journal Atmos. Chem. Phys.
Discussion started: 10 November 2017

Atmospheric Chemistry and Physics Discussions

212 $$\alpha = (1 + \frac{(k_7 + k_9 \cdot HO_2 / O_3) \cdot k_6 \cdot k_1 \cdot M \cdot O_2 + k_1 \cdot k_3 \cdot k_7 \cdot O_3 + 2 \cdot k_1 \cdot k_7 \cdot k_8 \cdot HO_2}{k_4 \cdot k_6 \cdot k_2}) / (1 + \frac{k_3 \cdot O_3 + 2 \cdot k_8 \cdot HO_2}{k_6 \cdot M \cdot O_2}).$$

213 Figure 1 shows height–latitude cross-sections of $< F(OH, HO_2, O_3) >$ for each month (in this
214 Section angle brackets denote monthly averaged zonal mean values). The dashed area
215 corresponds to χ > 85°. One can see that eq. (14) is most accurate within the 50–80 km range and
216 above 90 km, where $|< F > -1| \le 1\%$. The difference reaches 3–4 % in the region between 80 km
217 and 90 km. The altitude of this region has an annual variation with a maximum deviation in the
218 winter hemisphere. Below 50 km the value of $< F >$ sharply drops down to 0.25–0.30 at 40 km (not
219 shown in Fig. 1), thus below the stratopause Eq. (14) no longer describes simultaneous
220 photochemical equilibrium of OH, HO_2 and O_3.
221
222 **4. Method of statistical evaluation of simultaneous measurement of OH, HO_2 and O_3**
223
224 The proposed method is based on the statistical Bayesian procedure described in the works by
225 Kulikov et al. (2009) and Nechaev et al. (2016). It was originally developed for retrieving trace gas
226 concentrations in the mesosphere from ground-based and satellite measurements of other
227 mesospheric components. With respect to the considered evaluation problem this procedure
228 consists of three steps: (1) constructing conditional probability density function (PDF) of OH, HO_2
229 and O_3 concentration values at each altitude *z* in the selected interval assuming that there is
230 certain measurement data of these components and the algebraic relationship (14) is valid; (2)
231 calculating the first moments of this distribution, i.e. expected value and dispersion of each
232 component using the Metropolis-Hastings algorithm (Chib and Greenberg, 1995) for
233 multidimensional integration; (3) comparing the obtained results with the initial measurement data.
234 For constructing posterior PDF it is convenient to introduce vector $\vec{u}\{HO_2^r, O_3^r, OH^r\}$, whose
235 components are the retrieved values of chemical species concentrations at a certain *z*, and vector
236 $\vec{x}\{HO_2^m, O_3^m, OH^m\}$ composed of experimentally measured values of the components of vector $\vec{u}$,
237 $x_j = u_j + \xi_j$, $j = 1..3$, where ξ_j is a random error of measuring the *j*-th component of vector $\vec{u}$ at the
238 altitude *z*. It is assumed that
239 (1) random variables ξ_j are distributed normally with densities

Atmos. Chem. Phys. Discuss., https://doi.org/10.5194/acp-2017-738
Manuscript under review for journal Atmos. Chem. Phys.
Discussion started: 10 November 2017

Atmospheric Chemistry and Physics Discussions

$$w_j(\xi_j) = \frac{1}{\sqrt{2\pi}\sigma_j} exp\left(-\frac{\xi_j^2}{2\sigma_j^2}\right); \quad (15)$$

(2) ξ_j are mutually independent:

$$\vec{\xi}\{\xi_1, \xi_2, \xi_3\} \sim W_{\xi}(\vec{\xi}) = \prod_j w_j(\xi_j), \quad (16)$$

where $W_{\xi}(\vec{\xi})$ is the total PDF of all ξ_j;

(3) dispersions σ_j in Eq. (15), that are expected error values, are assumed to be known a priori (in our case they are provided by the MLS retrieval algorithm along with measured data).

Then the probability to observe vector $\vec{x}$ is given by the conditional PDF

$$P_x(\vec{x} \mid \vec{u}) = \int \delta(\vec{x} - \vec{u}) W_{\xi}(\vec{\xi}') d^3\vec{\xi}' = W_{\xi}(\vec{x} - \vec{u}), \quad (17)$$

where $\delta(\ldots)$ is delta function.

The prior relationship of HO_2^r, O_3^r and OH^r concentrations (Eq. (14)) can be written as $u_3 = G(u_1, u_2)$. Integrating the left-hand side of Eq. (17) with conditional PDF of the variable u_3:

$$P_{u_3}(u_3 \mid u_1, u_2) = \delta(u_3 - G(u_1, u_2)),$$

yields a likelihood function of the model

$$P_x(\vec{x} \mid u_1, u_2) = w_3(x_3 - G(u_1, u_2)) \cdot w_1(x_1 - u_1) w_2(x_2 - u_2). \quad (18)$$

According to Bayes' theorem, the posterior function, i.e. the probability density of latent variables u_1 and u_2, under the condition that $\vec{x}$ is observed, is defined by the expression

$$P(u_1, u_2 \mid \vec{x}) \propto P_x(\vec{x} \mid u_1, u_2) \cdot P_{apr}(u_1, u_2)$$
$$\propto exp\left(-\frac{(x_1 - u_1)^2}{2\sigma_1^2}\right) \cdot exp\left(-\frac{(x_2 - u_2)^2}{2\sigma_2^2}\right) \cdot exp\left(-\frac{(x_3 - G(u_1, u_2))^2}{2\sigma_3^2}\right) \cdot P_{apr}(u_1, u_2) \quad (19)$$

in which $P_{apr}(u_1, u_2)$ defines prior PDF of u_1 and u_2.

The retrieved value of the latent variable $u_{1,2,3}$ is hereinafter understood as the mean value of the function in Eq. (19):

Atmos. Chem. Phys. Discuss., https://doi.org/10.5194/acp-2017-738
Manuscript under review for journal Atmos. Chem. Phys.
Discussion started: 10 November 2017

Atmospheric Chemistry and Physics Discussions

$$\langle u_{1,2}\rangle = \int_{-\infty}^{\infty}\int_{-\infty}^{\infty} u_{1,2}\cdot P(u_1,u_2\,|\,\vec{x})du_1du_2$$

$$\langle u_3\rangle = \int_{-\infty}^{\infty}\int_{-\infty}^{\infty} G(u_1,u_2)\cdot P(u_1,u_2\,|\,\vec{x})du_1du_2. \quad (20)$$

Its dispersion defines the uncertainty of the retrieval:

$$\sigma_{u_j} = \sqrt{\langle u_j^2\rangle - \langle u_j\rangle^2},\ j=1..3, \quad (21)$$

where the angle brackets denote averaging in the sense of Eq. (20).

5. MLS/Aura data evaluation and results

We used the results of simultaneous measurement of trace gas concentrations and air temperature $T^{MLS}(p)$ obtained with MLS/ Aura (Wang et al., 2015a,b; Schwartz et al., 2015) within the 10^0 – 10^{-2} hPa air pressure interval. We took the daytime data when the solar zenith angle $\chi < 80°$ for January, May, and September 2005. The integrals in Eq. (20)–(21) were calculated at every pressure level p for each set of simultaneously measured vertical profiles $OH^{MLS}(p)$, $HO_2^{MLS}(p)$, $O_3^{MLS}(p)$, $T^{MLS}(p)$, $\sigma_{OH^{MLS}}(p)$, $\sigma_{HO_2^{MLS}}(p)$, $\sigma_{O_3^{MLS}}(p)$. The vertical profiles $<OH^r>(p)$, $<HO_2^r>(p)$, $<O_3^r>(p)$, $\sigma_{OH^r}(p)$, $\sigma_{HO_2^r}(p)$, $\sigma_{O_3^r}(p)$ were found at each point of the globe along the satellite track. Numerical integration was performed by a Monte Carlo method. For each pressure level, a sample of about $5\cdot10^5$ pairs of random variable values $\{u_1, u_2\} = \{HO_2^r, O_3^r\}$ distributed with normalized probability density given by Eq. (19) with $P_{apr}(u_1,u_2)\equiv 1$ was generated with the help of the Metropolis-Hastings algorithm (Chib and Greenberg, 1995). In this case, the statistical moments in Eq. (20)–(21) were determined by summation over the sample.

A typical example of retrieved profiles HO_2^r, O_3^r and OH^r (black curves) in comparison with the measured HO_2^{MLS}, O_3^{MLS} and OH^{MLS} (red curves) is given in Fig. 2. First of all, note that statistics of the retrieved data is in satisfactory agreement with the initial measurement of OH and O_3 concentrations, but not of HO_2. The error of satellite measurement, $\sigma_{HO_2^{MLS}}$, greatly exceeds the uncertainty of retrieval, $\sigma_{HO_2^r}$, so at some altitudes the values of $<HO_2^{MLS}>$ (red dashed curves) do

Atmos. Chem. Phys. Discuss., https://doi.org/10.5194/acp-2017-738
Manuscript under review for journal Atmos. Chem. Phys.
Discussion started: 10 November 2017

Atmospheric Chemistry and Physics Discussions

not fall within the corresponding intervals $< HO_2^r > \pm \sigma_{HO_2^r}$. Second, the results of a single measurement of all three components and their retrieved values have considerable uncertainties relative to their means within the whole interval of altitudes. Therefore, the observed and retrieved data should be compared using the commonly accepted approach (e.g., Pickett et al., 2008) of averaging large ensembles of profiles within certain latitude and time ranges, or zones. It is supposed that the noise of satellite measurement instruments is delta-correlated, so that random values corresponding to each single measured or retrieved profile are statistically independent. In this case the dispersion of a measured or retrieved zonal mean profile is determined by summation

$$\sigma^2{}_\Sigma = \frac{1}{N^2}\sum_{k=1}^{N}\sigma^2{}_k ,$$

where N is the number of measured or retrieved profiles within the zone and $\sigma^2{}_k$ is the dispersion of the k-th measured or retrieved profile.

The range of latitudes ±82° N covered by the satellite trajectory was divided into 16 equal zones. About 3000 single profiles of each chemical component fall into one zone during each month of MLS/Aura observations. Therefore, the resulting uncertainties of OH, HO_2 and O_3 concentration profiles (both measured and retrieved) averaged over such ensembles are significantly (about one and a half order of magnitude) lower than the uncertainties of individual profiles. Examples of such profiles for January, May and September 2005 are presented in Fig. 3. One can see that the indicated uncertainties are now small enough to make clear conclusions about the extent to which the observed and retrieved profiles agree by comparing their averaged values only, i.e. $< OH^{MLS} >$, $< HO_2^{MLS} >$, $< O_3^{MLS} >$ and $< OH^r >$, $< HO_2^r >$, $< O_3^r >$.

Figures 4–6 show monthly averaged zonal mean pressure–latitude cross-sections of $< HO_2^r >$, $< HO_2^{MLS} >$, $\Delta HO_2 = (< HO_2^r > - < HO_2^{MLS} >)/ < HO_2^{MLS} >$ and similar characteristics for OH and O_3 concentration profiles for three months of the year 2005. First, clearly, the distributions of $< OH^r >$ and $< O_3^r >$ are in good qualitative and quantitative agreement with the initial MLS/Aura measurement data at lower altitudes, below ~ 0.1 hPa. At higher altitudes, the distributions of $< OH^r >$ reproduce all the main structural features of $< OH^{MLS} >$ except for a small 2–3 km downward displacement of the OH layer. Moreover, at these altitudes the retrieved OH concentration has lower values than the observed one with a relative difference ΔOH reaching

Atmos. Chem. Phys. Discuss., https://doi.org/10.5194/acp-2017-738
Manuscript under review for journal Atmos. Chem. Phys.
Discussion started: 10 November 2017

several tens of percent at altitudes above ~ 0.05 hPa. The distribution of $<O_3^r>$ above 0.1 hPa, in turn, differs considerably from $<O_3^{MLS}>$, both in quantity and quality, especially within the 0.003–0.05 hPa altitude interval, where ΔO_3 locally reaches several times. Second, for all months there are significant qualitative and quantitative differences between $<HO_2^r>$ and $<HO_2^{MLS}>$, the most noticeable one being location of the mesospheric maximum of this component's concentration. According to the observations it is close to 0.1 hPa, while the retrieved data demonstrates the altitude of about 0.05 hPa.

6. Discussion and conclusion

On the basis of the data presented in Section 5 we can conclude that, upon the whole, simultaneous OH, HO_2 and O_3 satellite measurements poorly satisfy the photochemical equilibrium condition. The HO_2 component biases from this condition most prominently. We can conjecture that a possible explanation for the bias is significant systematic error in HO_2 measurements, in particular, in the height of mesospheric maximum. The discrepancy between the measured and real HO_2, in turn, impacts the retrieved data for OH and O_3 and, above 0.1 hPa, leads to a significant mismatch between the averaged retrieved values ($<OH^r>$, $<O_3^r>$) and averaged measured values ($<OH^{MLS}>$, $<O_3^{MLS}>$).

EOS MLS data quality and description document (Livesey et al., 2017) states that scientifically useful pressure range for HO_2 measurements is 22 – 0.046 hPa. Exclusion from Figs. 4-6 of the range above 0.046 hPa diminishes the mismatch for OH and O_3 but not for HO_2. An algorithm for offline retrieval of daily zonal means of HO_2 using averaged MLS radiances was performed by Millán et al. (2015). The product of the algorithm, the alternative dataset of night-time and daytime HO_2, recently became available at https://mls.jpl.nasa.gov. Figure 7 shows the monthly averaged zonal means from the dataset ($<HO_2^{MLS}{}_{offline}>$) corresponding to Figs. 4-6. Figure 7 depicts the same monthly means as Figures 4-6. One can see that the results of the offline HO_2 retrieval show the same features as the results of our evaluation technique as compared to standard MLS retrieval: the height of mesospheric HO_2 maximum is higher. It is worth noting that the positions of the maximum in $<HO_2^r>$ and $<HO_2^{MLS}{}_{offline}>$ distributions are close.

For detailed qualitative and quantitative comparison of $< HO_2^r >$ and $< HO_2^{MLS}{}_{offline} >$ one should use the evaluation procedure technique for zonally averaged all three MLS components, which requires significant modification of the procedure and is beyond the scope of this technical Note.

The proposed method for evaluation of mesospheric species measurements can be readily generalized to other atmospheric photochemical systems that contain short lifetime components (see the Introduction). It may also be modified for assessing hard to measure chemical components, characteristics of atmospheric processes (like wind speed or turbulent diffusion rate), or poorly known reaction rates. Such evaluation will be correct from the statistical point of view.

Acknowledgments

This work was supported by the Russian Science Foundation (contract No. 15–17–10024 of June 04, 2015). The data used in this study is supported by the Institute of Applied Physics of the Russian Academy of Sciences (Nizhny Novgorod, Russia). Inquiries about calculated distributions used for this paper can be addressed to Mr. Belikovich (belikovich@ipfran.ru).

References

Avallone, L. M., and Toohey, D. W.: Tests of halogen photochemistry using in situ measurements of ClO and BrO in the lower polar stratosphere, J. Geophys. Res., Volume 106, Issue D10, Pages 10411–1042, doi: 10.1029/2000JD900831, 2001.

Benton, A. K., Langridge, J. M., Ball, S. M., Bloss, W. J., Dall'Osto, M., Nemitz, E., Harrison, R. M., and Jones, R. L.: Night-time chemistry above London: measurements of NO3 and N2O5 from the BT Tower, Atmos. Chem. Phys., 10, 9781-9795, doi:10.5194/acp-10-9781-2010, 2010.

Berthet, G., Ricaud, P., Lefevre, F., Le Flochmoen, E., Urban, J., Barret, B., Lautie, N., Dupuy, E., De La Noe, J., and Murtagh, D.: Nighttime chlorine monoxide observations by the Odin satellite and implications for the ClO/Cl_2O_2 equilibrium, Geophys. Res. Lett., 32, L11812, doi:10.1029/2005GL022649, 2005.

Brown, S. S., Stark, H., Ryerson, T. B., Williams, E. J., Nicks Jr., D. K., Trainer, M., Fehsenfeld, F. C., and Ravishankara, A. R.: Nitrogen oxides in the nocturnal boundary layer: Simultaneous in situ measurements of NO_3, N_2O_5, NO_2, NO, and O_3, J. Geophys. Res., 108(D9), 4299, doi:10.1029/2002JD002917, 2003.

Butz, A., H. Bosch, C. Camy-Peyret, M. Dorf, A. Engel, S. Payan, and Pfeilsticker, K.: Observational constraints on the kinetics of the ClO-BrO and ClO-ClO ozone loss cycles in the Arcticwinter stratosphere, Geophys. Res. Lett., 34, L05801, doi:10.1029/2006GL028718, 2007.

Cantrell, C. A., Mauldin, L., Zondlo, M., Eisele, F., Kosciuch, E., Shetter, R., Lefer, B., Hall, S., Campos, T., Ridley, B., Walega, J., Fried, A., Wert, B., Flocke, F., Weinheimer, A., Hannigan, J., Coffey, M., Atlas, E., Stephens, S., Heikes, B., Snow, J., Blake, D., Blake, N., Katzenstein, A., Lopez, J., Browell, E. V., Dibb, J., Scheuer, E., Seid, G., and Talbot, R.: Steady state free radical budgets and ozone photochemistry during TOPSE, J. Geophys. Res., 108(D4), 8361, doi:10.1029/2002JD002198, 2003.

Chameides, W.: Tropospheric odd nitrogen and the atmospheric water vapor cycle, J. Geophys. Res., 84 (C10), 4989–4996, doi: 10.1029/JC080i036p04989, 1975.

Chib, S., and Greenberg, E.: Understanding the Metropolis-Hastings Algorithm, The American Statistician, 49 (4), 327-335, doi: 10.2307/2684568, 1995.

Crawford, J., Davis, D., Chen, G., Bradshaw, J., Sandholm, S., Gregory, G., Sachse, G., Anderson, B., Collins, J., Blake, D., Singh, H., Heikes, B., Talbot, R., Rodriguez, J.: Photostationary state analysis of the NO_2-NO system based on airborne observations from the western and central North Pacific, 101(D1), 2053–2072, doi: 10.1029/95JD02201, 1996.

Crowley, J. N., Schuster, G., Pouvesle, N., Parchatka, U., Fischer, H., Bonn, B., Bingemer, H., and Lelieveld, J.: Nocturnal nitrogen oxides at a rural mountain-site in south-western Germany, Atmos. Chem. Phys., 10, 2795-2812, doi:10.5194/acp-10-2795-2010, 2010.

de Grandpre, J., Beagley, S. R., Fomichev, V. I., Griffioen, E., McConnell, J. C., Medvedev, A. S., and Shepherd., T. G.: Ozone climatology using interactive chemistry: Results from the Canadian Middle Atmosphere Model, J. Geophys. Res.-Atmos., 105, 26475-26491, doi:10.1029/2000JD900427, 2000.

Djouad, R., Michelangeli, D. V., and Gong, W.: Numerical solution for atmospheric multiphase models: Testing the validity of equilibrium assumptions, J. Geophys. Res., 108(D19), 4602, doi:10.1029/2002JD002969, 2003.

Douglass, A. R., Jackman, C. H., and Stolarski, R. S.: Comparison of model results transporting the odd nitrogen family with results transporting separate odd nitrogen species, J. Geophys. Res., 94(D7), 9862–9872, doi:10.1029/JD094iD07p09862, 1989.

Evans, W. F. J., and Llewellyn, E. J.: Atomic hydrogen concentrations in the mesosphere and the hydroxyl emissions, J. Geophys. Res., 78, 323–326, doi:10.1029/JA078i001p00323, 1973.

Evans, W.F.J., McDade, I. C., Yuen, J., and Llewellyn, E. J.: A rocket measurement of the O_2 infrared atmospheric (0-0) band emission in the dayglow and a determination of the mesospheric ozone and atomic oxygen densities, Can. J. Phys., 66, 941–946, doi:10.1139/p88-15, 1988.

Feigin, A. M., and Konovalov, I. B.: On the possibility of complicated dynamic behavior of atmospheric photochemical systems: Instability of the Antarctic photochemistry during the ozone hole formation, J. Geophys. Res., 101, 26023–26038, doi:10.1029/96JD02011, 1996.

Feigin, A. M., Konovalov, I. B., and Molkov, Ya. I.: Towards understanding nonlinear nature of atmospheric photochemistry: Essential dynamic model of the mesospheric photochemical system, J. Geophys. Res., 103, 25447–25460, doi:10.1029/98JD01569, 1998.

Funke, B., Lopez-Puertas, M., von Clarmann, T., Stiller, G. P., Fischer, H., Glatthor, N., Grabowski, U., Hopfner, M., Kellmann, S., Kiefer, M., Linden, A., Mengistu Tsidu, G., Milz, M., Steck, T. and Wang, D. Y.: Retrieval of stratospheric NOx from 5.3 and 6.2 mm nonlocal thermodynamic equilibrium emissions measured by Michelson Interferometer for Passive Atmospheric Sounding (MIPAS) on Envisat, J. Geophys. Res., 110, D09302, doi:10.1029/2004JD005225, 2005.

Ghosh, S., Pyle, J. A., and Good, P.: Temperature dependence of the ClO concentration near the stratopause, J. Geophys. Res., 102(D15), 19207–19216, doi:10.1029/97JD01099, 1997.

Good, R. E.: Determination of atomic oxygen density from rocket borne measurements of hydroxyl airglow, Planet. Space Sci., 24, 389–395, doi.org/10.1016/0032-0633(76)90052-0, 1976.

Grygalashvyly, M.: Several notes on the OH* layer, Ann. Geophys., 33, 923-930, doi:10.5194/angeo-33-923-2015, 2015.

Grygalashvyly, M., Sonnemann, G. R., and Hartogh, P.: Long-term behavior of the concentration of the minor constituents in the mesosphere—A model study, Atmos. Chem. Phys., 9, 2779–2792, doi:10.5194/acp-9-2779-2009, 2009.

Grygalashvyly, M., Becker, E., and Sonnemann, G. R.: Wave mixing effects on minor chemical constituents in the MLT region: Results from a global CTM driven by high-resolution dynamics, J. Geophys. Res., 116, D18302, doi:10.1029/2010JD015518, 2011.

Grygalashvyly, M., Becker, E., and Sonnemann, G. R.: Gravity wave mixing and effective diffusivity for minor chemical constituents in the mesosphere/lower thermosphere, Space Sci. Rev., 168, 333–362, doi:10.1007/s11214-011-9857-x, 2012.

Grygalashvyly, M., Sonnemann, G. R., Lübken, F.-J., Hartogh, P., and Berger, U.: Hydroxyl layer: Mean state and trends at midlatitudes, J. Geophys. Res.-Atmos., 119, 12391–12419, doi:10.1002/2014JD022094, 2014.

Hartogh, P., Jarchow, C., Sonnemann, G. R., and Grygalashvyly, M.: On the spatiotemporal behavior of ozone within the upper mesosphere/mesopause region under nearly polar night conditions, J. Geophys. Res., 109, D18303, doi:10.1029/2004JD004576, 2004.

Hartogh, P., Sonnemann, G. R., Grygalashvyly, M., and Jarchow, Ch.: Ozone trends in mid-latitude stratopause region based on microwave measurements at Lindau (51.66° N, 10.13° E), the ozone reference model, and model calculations, Adv. Space Res., 47, 1937-1948, doi:10.1016/j.asr.2011.01.010, 2011.

Hauchecorne, A., Bertaux, J. L., Dalaudier, F., Keckhut, P., Lemennais, P., Bekki, S., Marchand, M., Lebrun, J. C., Kyrölä, E., Tamminen, J., Sofieva, V., Fussen, D., Vanhellemont, F., Fanton d'Andon, O., Barrot, G., Blanot, L., Fehr, T., and Saavedra de Miguel, L.: Response of tropical stratospheric O_3, NO_2 and NO_3 to the equatorial Quasi-Biennial Oscillation and to temperature as seen from GOMOS/ENVISAT, Atmos. Chem. Phys., 10, 8873-8879, doi:10.5194/acp-10-8873-2010, 2010.

Kawa, S. R., Fahey, D. W., Solomon, S., Brune, W. H., Proffitt, M. H., Toohey, D. W., Anderson Jr., D. E., Anderson, L. C., and Chan, K. R.: Interpretation of aircraft measurements of NO, ClO, and O_3 in the lower stratosphere, J. Geophys. Res., 95(D11), 18597–18609 doi: 10.1029/JD095iD11p18597, 1990.

Kaye, J. A., and Rood, R. B.: Chemistry and transport in a three-dimensional stratospheric model: Chlorine species during a simulated stratospheric warming, J. Geophys. Res., 94(D1), 1057–1083, doi: 10.1029/JD094iD01p01057, 1989.

Ko, M., Hu, W., Rodriguez, J. M., Kondo, Y., Koike, M., Kita, K., Kawakami, S., Blake, D., Liu, S., and Ogawa, T.: Photochemical ozone budget during the BIBLE A and B campaigns, J. Geophys. Res., 107, 8404, doi:10.1029/2001JD000800, 2002. [printed 108(D3), 2003].

461 Kondo, Y., Matthews, W. A., Aimedieu, P., and Robbins, D. E. Diurnal variation of nitric
462 oxide at 32 km: Measurements and interpretation, J. Geophys. Res., 93(D3), 2451–2460,
463 doi:10.1029/JD093iD03p02451, 1988.
464 Kondo, Y., Ziereis, H., Koike, M., Kawakami, S., Gregory, G. L., Sachse, G. W., Singh, H.
465 B., Davis, D. D., Merrill, J. T.: Reactive nitrogen over the Pacific Ocean during PEM-West, A
466 101(D1), 1809–1828, doi:10.1029/95JD02611, 1996.
467 Konovalov, I. B., Feigin, A. M., Mukhina, A. Y.: Toward understanding of the nonlinear
468 nature of atmospheric photochemistry: Multiple equilibrium states in the high-latitude lower
469 stratospheric photochemical system, J. Geophys. Res, 104, 8669-8689,
470 doi:10.1029/1998JD100037, 1999.
471 Konovalov, I. B., and Feigin, A. M.: Toward an understanding of the nonlinear nature of
472 atmospheric photochemistry: Origin of the complicated dynamic behaviour of the mesospheric
473 photochemical system, Nonlin. Processes Geophys., 7, 87–104, doi:10.5194/npg-7-87-2000, 2000.
474 Körner, U., and Sonnemann, G. R.: Global 3D-modeling of water vapor concentration of the
475 mesosphere/mesopause region and implications with respect to the NLC region, J. Geophys. Res.-
476 Atmos., 106, 9639– 9651, doi:10.1029/2000JD900744, 2001.
477 Kowalewski, S., von Savigny, C., Palm, M., McDade, I. C., and Notholt, J.: On the impact of
478 the temporal variability of the collisional quenching process on the mesospheric OH emission layer:
479 a study based on SD-WACCM4 and SABER, Atmos. Chem. Phys., 14, 10193-10210,
480 doi:10.5194/acp-14-10193-2014, 2014.
481 Kremser, S., Schofield, R., Bodeker, G. E., Connor, B. J., Rex, M., Barret, J., Mooney, T.,
482 Salawitch, R. J., Canty, T., Frieler, K., Chipperfield, M. P., Langematz, U., and Feng, W.: Retrievals
483 of chlorine chemistry kinetic parameters from Antarctic ClO microwave radiometer measurements,
484 Atmos. Chem. Phys., 11, 5183-5193, doi:10.5194/acp-11-5183-2011, 2011.
485 Kulikov, M. Y., Feigin, A. M., and Sonnemann, G. R.: Retrieval of the vertical distribution of
486 chemical components in the mesosphere from simultaneous measurements of ozone and hydroxyl
487 distributions, Radiophys. Quantum Electron., 49, 683–691, doi:10.1007/s11141-006-0103-4, 2006.
488 Kulikov, M. Yu., Feigin, A. M., and Sonnemann, G. R.: Retrieval of water vapor profile in the
489 mesosphere from satellite ozone and hydroxyl measurements by the basic dynamic model of
490 mesospheric photochemical system, Atmos. Chem. Phys., 9, 8199-8210, doi:10.5194/acp-9-8199-
491 2009, 2009.

Kulikov, M. Y., Mukhin, D. N., and Feigin, A. M.: Bayesian strategy of accuracy estimation for characteristics retrieved from experimental data using base dynamic models of atmospheric photochemical systems, Radiophys. Quantum Electron., 52, 618–626, doi:10.1007/s11141-010-9171-6, 2009.

Kulikov, M. Yu., Vadimova, O. L., Ignatov, S. K., and Feigin, A.M.: The mechanism of non-linear photochemical oscillations in the mesopause region, Nonlinear Processes in Geophysics, v.19, p.p.501–512, doi:10.5194/npg-19-501-2012, 2012.

Kulikov, M. Yu., and Feigin, A. M.: Automated construction of the basic dynamic models of the atmospheric photochemical systems using the RADM2 chemical mechanism as an example, Radiophys. Quantum Electron., 57, 478-487, doi 10.1007/s11141-014-9530-9, 2014.

Kulikov, M. Y., Belikovich, M. V., Grygalashvyly, M., Sonnemann, G. R., Ermakova, T. S., Nechaev, A. A., and Feigin, A. M.: Daytime ozone loss term in the mesopause region, Ann. Geophys., 35, 677-682, doi:10.5194/angeo-35-677-2017, 2017.

Livesey, N. J., et al., EOS MLS version 4.2x Level 2 data quality and description document, Tech. rep., Jet Propulsion Laboratory, D-33509 Rev. C, available from https://mls.jpl.nasa.gov/data/v4-2_data_quality_document.pdf, 2017.

Llewellyn, E. J., McDade, I. C., Moorhouse, P., and Lockerbie, M. D.: Possible reference models for atomic oxygen in the terrestrial atmosphere, Adv. Space Res., 13, 135–144, doi:0.1016/0273-1177(93)90013-2, 1993.

Llewellyn, E. J., and McDade, I. C.: A reference model for atomic oxygen in the terrestrial atmosphere, Adv. Space Res., 18, 209–226, doi:10.1016/0273-1177(96)00059-2, 1996.

Marchand, M., Bekki, S., Lefevre, F., and Hauchecorne, A.: Temperature retrieval from stratospheric O3 and NO3 GOMOS data, Geophys. Res. Lett., 34, L24809, doi:10.1029/2007GL030280, 2007.

Marsh, D. R., Smith, A. K., Mlynczak, M. G., and Russell III, J. M.: SABER observations of the OH Meinel airglow variability near the mesopause, J. Geophys. Res., 111, A10S05, doi:10.1029/2005JA011451, 2006.

Martinez, M., Perner, D., Hackenthal, E.-M., Kulzer, S., and Schultz, L.: NO_3 at Helgoland during the NORDEX campaign in October 1996, J. Geophys. Res., 105(D18), 22,685–22,695, doi:10.1029/2000JD900255, 2000.

Massie, S. T., and Hunten, D. M.: Stratospheric eddy diffusion coefficients from tracer data, J. Geophys. Res., 86(C10), 9859–9868, doi:10.1029/JC086iC10p09859, 1981.

McDade, I. C., Llewellyn, E. J., and Harris, F. R.: Atomic oxygen concentrations in the lower auroral thermosphere, Adv. Space Res., 5(7), 229–232, doi:10.1016/0273-1177(85)90379-5, 1985.

McDade, I. C., and Llewellyn, E. J.: Mesospheric oxygen atom densities inferred from night-time OH Meinel band emission rates, Planet. Space Sci., 36, 897–905, DOI:10.1016/0032-0633(88)90097-9, 1988.

McLaren, R., Wojtal, P., Majonis, D., McCourt, J., Halla, J. D., and Brook, J.: NO_3 radical measurements in a polluted marine environment: links to ozone formation, Atmos. Chem. Phys., 10, 4187-4206, doi:10.5194/acp-10-4187-2010, 2010.

Millán, L., Wang, S., Livesey, N., Kinnison, D., Sagawa, H., and Kasai, Y.: Stratospheric and mesospheric HO_2 observations from the Aura Microwave Limb Sounder, Atmos. Chem. Phys., 15, 2889-2902, doi:10.5194/acp-15-2889-2015, 2015.

Mlynczak, M. G., and Solomon, S.: Middle atmosphere heating by exothermic chemical reactions involving odd-hydrogen species, Geophys. Res. Lett., 18, 37-40, doi:10.1029/90GL02672, 1991.

Mlynczak, M. G., and Solomon, S.: A detailed evaluation of the heating efficiency in the middle atmosphere, J. Geophys. Res., 98, 10,517–10,541, doi:10.1029/93JD00315, 1993.

Mlynczak, M. G., Marshall, B. T., Martin-Torres, F. J., Russell III, J. M., Thompson, R. E., Remsberg, E. E., and Gordley, L. L.: Sounding of the Atmosphere using Broadband Emission Radiometry observations of daytime mesospheric O2(1D) 1.27 μm emission and derivation of ozone, atomic oxygen, and solar and chemical energy deposition rates, J. Geophys. Res., 112, D15306, doi:10.1029/2006JD008355, 2007.

Mlynczak, M. G., Hunt, L. A., Mast, J. C., Marshall, B. T., Russell III, J. M., Smith, A. K., Siskind, D. E., Yee, J.-H., Mertens, C. J., Martin-Torres, F. J., Thompson, R. E., Drob, D. P., and Gordley, L. L.: Atomic oxygen in the mesosphere and lower thermosphere derived from SABER: Algorithm theoretical basis and measurement uncertainty, J. Geophys. Res., 118, 5724–5735, doi:10.1002/jgrd.50401, 2013a.

Mlynczak, M. G., Hunt, L. H., Mertens, C. J., Marshall, B. T., Russell III, J. M., López-Puertas, M., Smith, A. K., Siskind, D. E., Mast, J. C., Thompson, R. E., and Gordley, L. L.:

552 Radiative and energetic constraints on the global annual mean atomic oxygen concentration in the
553 mesopause region, J. Geophys. Res. Atmos., 118, 5796–5802, doi:10.1002/jgrd.50400, 2013b.
554 Mlynczak, M. G., Hunt, L. A., Marshall, B. T., Mertens, C. J., Marsh, D. R., Smith, A. K.,
555 Russell, J. M., Siskind, D. E., and Gordley, L. L.: Atomic hydrogen in the mesopause region
556 derived from SABER: Algorithm theoretical basis, measurement uncertainty, and results, J.
557 Geophys. Res., 119, 3516–3526, doi:10.1002/2013JD021263, 2014.
558 Nechaev, A. A., Ermakova, T. S., and Kulikov, M. Y.: Determination of the Trace-Gas
559 Concentrations at the Altitudes of the Lower and Middle Mesosphere from the Time Series of
560 Ozone Concentration, Radiophys. Quantum Electron., 59, 546–559, doi:10.1007/s11141-016-
561 9722-6, 2016.
562 Nikoukar, R., Swenson, G. R., Liu, A. Z., and Kamalabadi, F.: On the variability of
563 mesospheric OH emission profiles, J. Geophys. Res., 112, D19109, doi:10.1029/2007JD008601,
564 2007.
565 Pendleton, W. R., Baker, K. D., and Howlett, L. C.: Rocket-based investigations of $O(^3P)$,
566 $O_2(a^1\Delta_g)$ and OH*(ν=1,2) during the solar eclipse of 26 February1979, J. Atm. Terr. Phys., 45 (7),
567 479 – 491, doi:10.1016/S0021-9169(83)81108-8, 1983.
568 Penkett, S. A., Monks, P. S., Carpenter, L. J., Clemitshaw, K. C., Ayers, G. P., Gillett, R. W.,
569 Galbally, I. E., and Meyer, C. P.: Relationships between ozone photolysis rates and peroxy radical
570 concentrations in clean marine air over the Southern Ocean, J. Geophys. Res., 102(D11), 12805–
571 12817, doi:10.1029/97JD00765, 1997.
572 Penkett, S. A., Reeves, C. E., Bandy, B. J., Kent, J. M., and Richer, H. R.: Comparison of
573 calculated and measured peroxide data collected in marine air to investigate prominent features of
574 the annual cycle of ozone in the troposphere, J. Geophys. Res., 103(D11), 13377–13388,
575 doi:10.1029/97JD02852, 1998.
576 Platt, U., Perner, D., and Pätz, H. W.: Simultaneous measurement of atmospheric CH2O,
577 O3, and NO2 by differential optical absorption, J. Geophys. Res., 84(C10), 6329–6335,
578 10.1029/JC084iC10p06329, 1979.
579 Pyle, J. A., Zavody, A. M., Harries, J. E., and Moffat, P. H.: Derivation of OH concentration
580 from satellite infrared measurements of NO_2 and HNO_3, Nature, 305, 690-692,
581 doi:10.1038/305690a0, 1983.

582 Pyle, J. A., and Zavody, A. M.: The derivation of hydrogen containing radical concentrations
583 from satellite data sets, Q. J. R. Meteorol. Soc., 111, 993-1012, doi:10.1002/qj.49711147005,
584 1985.
585 Pickett, H. M., and Peterson, D. B.: Comparison of measured stratospheric OH with
586 prediction, J. Geophys. Res., 101(D11), 16789–16796, doi: 10.1029/96JD01168, 1996.
587 Pickett, H. M., Drouin, B. J., Canty, T., Salawitch, R. J., Fuller, R. A., Perun, V. S., Livesey,
588 N. J., Waters, J. W., Stachnik, R. A., Sander, S. P., Traub, W. A., Jucks, K. W., and Minschwaner,
589 K.: Validation of Aura Microwave Limb Sounder OH and HO2 measurements, J. Geophys. Res.,
590 113, D16S30, doi:10.1029/2007JD008775, 2008.
591 Rasch, P. J., Boville, B. A., and Brasseur, G. P.: A three-dimensional general circulation
592 model with coupled chemistry for the middle atmosphere, J. Geophys. Res., 100(D5), 9041–9071,
593 doi: 10.1029/95JD00019, 1995.
594 Russell, J. P., and Lowe, R. P.: Atomic oxygen profiles (80–94 km) derived from Wind
595 Imaging Interferometer/Upper Atmospheric Research Satellite measurements of the hydroxyl
596 airglow: 1. Validation of technique, J. Geophys. Res., 108, 4662, doi:10.1029/2003JD003454, D21,
597 2003.
598 Schwartz, M., Froidevaux, L., Livesey, N., and Read, W.: MLS/Aura Level 2 Ozone (O_3)
599 Mixing Ratio V004, Greenbelt, MD, USA, Goddard Earth Sciences Data and Information Services
600 Center (GES DISC), accessed 13.07.16, doi:10.5067/AURA/MLS/DATA2017, 2015.
601 Scinocca, J. F., McFarlane, N. A., Lazare, M., Li, J., Plummer, D.: The CCCma third
602 generation AGCM and its extension into the middle atmosphere, Atmos. Chem. Phys., 8, 7055-
603 7074, doi:10.5194/acp-8-7055-2008, 2008.
604 Siskind, D. E., Marsh, D. R., Mlynczak, M. G., Martin-Torres, F. J., and Russell III, J. M.:
605 Decreases in atomic hydrogen over the summer pole: Evidence for dehydration from polar
606 mesospheric clouds?, Geophys. Res. Lett., 35, L13809, doi:10.1029/2008GL033742, 2008.
607 Siskind D. E., Mlynczak, M. G., Marshall, T., Friedrich, M., Gumbel, J.: Implications of odd
608 oxygen observations by the TIMED/SABER instrument for lower D region ionospheric modeling, J.
609 Atmos. Sol. Terr. Phys., 124, 63–70, doi: 10.1016/j.jastp.2015.01.014, 2015.
610 Smith, A. K., Marsh, D. R., Mlynczak, M. G., and Mast, J. C.: Temporal variations of atomic
611 oxygen in the upper mesosphere from SABER, J. Geophys. Res., 115, D18309,
612 doi:10.1029/2009JD013434, 2010.

Sobanski, N., Tang, M. J., Thieser, J., Schuster, G., Pöhler, D., Fischer, H., Song, W., Sauvage, C., Williams, J., Fachinger, J., Berkes, F., Hoor, P., Platt, U., Lelieveld, J., and Crowley, J. N.: Chemical and meteorological influences on the lifetime of NO3 at a semi-rural mountain site during PARADE, Atmos. Chem. Phys., 16, 4867-4883, doi:10.5194/acp-16-4867-2016, 2016.

Sonnemann, G., Kremp, C., Ebel, A., and Berger, U.: A three-dimensional dynamic model of minor constituents of the mesosphere, Atmos. Environ., 32, 3157–3172, doi:10.1016/S1352-2310(98)00113-7, 1998.

Sonnemann, G. R., Grygalashvyly, M., Hartogh, P., and Jarchow, C.: Behavior of mesospheric ozone under nearly polar night conditions, Adv. Space Res., 38, 2402–2407, doi:10.1016/j.asr.2006.09.011, 2006a.

Sonnemann, G. R., Hartogh, P., Jarchow, C., Grygalashvyly, M., and Berger, U.: On the winter anomaly of the night-to-day ratio of ozone in the middle to upper mesosphere in middle to high latitudes, Adv. Space Res., 40, 846–854, doi:10.1016/j.asr.2007.01.039, 2007.

Sonnemann, G. R., Hartogh, P., Berger, U., and Grygalashvyly, M.: Hydroxyl layer: trend of number density and intra-annual variability Ann. Geophys., 33, 749–767, doi:10.5194/angeo-33-749-2015, 2015.

Swenson, G. R., and Gardner, C. S.: Analytical models for the responses of the mesospheric OH* and Na layers to atmospheric gravity waves, J. Geophys. Res., 103(D6), 6271–6294, doi:10.1029/97JD02985, 1998.

Solomon, P., Connor, B., Barrett, J., Mooney, T., Lee, A., and Parrish, A.: Measurements of stratospheric ClO over Antarctica in 1996–2000 and implications for ClO dimer chemistry, Geophys. Res. Lett., 29(15), 1708, doi:10.1029/2002GL015232, 2002.

Stedman, D. H., Chameides, W., and Jackson, J. O.: Comparison of experimental and computed values for J(NO_2), Geophys. Res. Lett., 2(1), 22-25, doi:1029/GL002i001p00022, 1975.

Stimpfle, R. M., Wilmouth, D. M., Salawitch, R. J., and Anderson, J. G.: First measurements of ClOOCl in the stratosphere: The coupling of ClOOCl and ClO in the Arctic polar vortex, J. Geophys. Res., 109, D03301, doi:10.1029/2003JD003811, 2004.

Sumińska-Ebersoldt, O., Lehmann, R., Wegner, T., Grooß, J.-U., Hösen, E., Weigel, R., Frey, W., Griessbach, S., Mitev, V., Emde, C., Volk, C. M., Borrmann, S., Rex, M., Stroh, F., and von Hobe, M.: ClOOCl photolysis at high solar zenith angles: analysis of the RECONCILE self-match flight, Atmos. Chem. Phys., 12, 1353-1365, doi:10.5194/acp-12-1353-2012, 2012.

644 Thomas, R. J.: Atomic hydrogen and atomic oxygen density in the mesosphere region:
645 Global and seasonal variations deduced from Solar Mesosphere Explorer near-infrared emissions,
646 J. Geophys. Res., 95, 16,457–16,476, doi:10.1029/JD095iD10p16457, 1990.
647 Tulet, P., Grini, A., Griffin, R. J., and Petitcol, S.: ORILAM-SOA: A computationally efficient
648 model for predicting secondary organic aerosols in three-dimensional atmospheric models, J.
649 Geophys. Res., 111, D23208, doi:10.1029/2006JD007152, 2006.
650 von Hobe, M., Grooß, J.-U., Müller, R., Hrechanyy, S., Winkler, U., and Stroh, F.: A re-
651 evaluation of the ClO/Cl2O2 equilibrium constant based on stratospheric in-situ observations,
652 Atmos. Chem. Phys., 5, 693-702, doi:10.5194/acp-5-693-2005, 2005.
653 von Hobe, M., Salawitch, R. J., Canty, T., Keller-Rudek, H., Moortgat, G. K., Grooß, J.-U.,
654 Müller, R., and Stroh, F.: Understanding the kinetics of the ClO dimer cycle, Atmos. Chem. Phys.,
655 7, 3055-3069, doi:10.5194/acp-7-3055-2007, 2007.
656 Wang, S., Pickett, H., Livesey, N., and Read, W.: MLS/Aura Level 2 Hydroperoxy (HO_2)
657 Mixing Ratio V004, Greenbelt, MD, USA, Goddard Earth Sciences Data and Information Services
658 Center (GES DISC), accessed 13.07.16, doi:10.5067/AURA/MLS/DATA2013, 2015a.
659 Wang, S., Livesey, N., and Read, W.: MLS/Aura Level 2 Hydroxyl (OH) Mixing Ratio V004,
660 Greenbelt, MD, USA, Goddard Earth Sciences Data and Information Services Center (GES DISC),
661 accessed 13.07.16, doi:10.5067/AURA/MLS/DATA2018, 2015b.
662 Webster, C. R., May, R. D., Toumi, R., and Pyle, J. A.: Active nitrogen partitioning and the
663 nighttime formation of N2O5 in the stratosphere: Simultaneous in situ measurements of NO, NO_2,
664 HNO_3, O_3, and N_2O using the BLISS diode laser spectrometer, J. Geophys. Res., 95(D9), 13851–
665 13866 doi: 10.1029/JD095iD09p13851, 1990.
666 Wetzel, G., Oelhaf, H., Kirner, O., Friedl-Vallon, F., Ruhnke, R., Ebersoldt, A., Kleinert, A.,
667 Maucher, G., Nordmeyer, H., and Orphal, J.: Diurnal variations of reactive chlorine and nitrogen
668 oxides observed by MIPAS-B inside the January 2010 Arctic vortex, Atmos. Chem. Phys., 12,
669 6581-6592, doi:10.5194/acp-12-6581-2012, 2012.
670 Xu, J., Smith, A. K., Jiang, G., Gao, H., Wei, Y., Mlynczak, M. G. ,and Russell III, J. M.:
671 Strong longitudinal variations in the OH nightglow, Geophys. Res. Lett., 37, L21801,
672 doi:10.1029/2010GL043972, 2010.

673 Xu, J., Gao, H., Smith, A. K., and Zhu, Y.: Using TIMED/SABER nightglow observations to
674 investigate hydroxyl emission mechanisms in the mesopause region, J. Geophys. Res., 117,
675 D02301, doi:10.1029/2011JD016342, 2012.
676

Atmos. Chem. Phys. Discuss., https://doi.org/10.5194/acp-2017-738
Manuscript under review for journal Atmos. Chem. Phys.
Discussion started: 10 November 2017

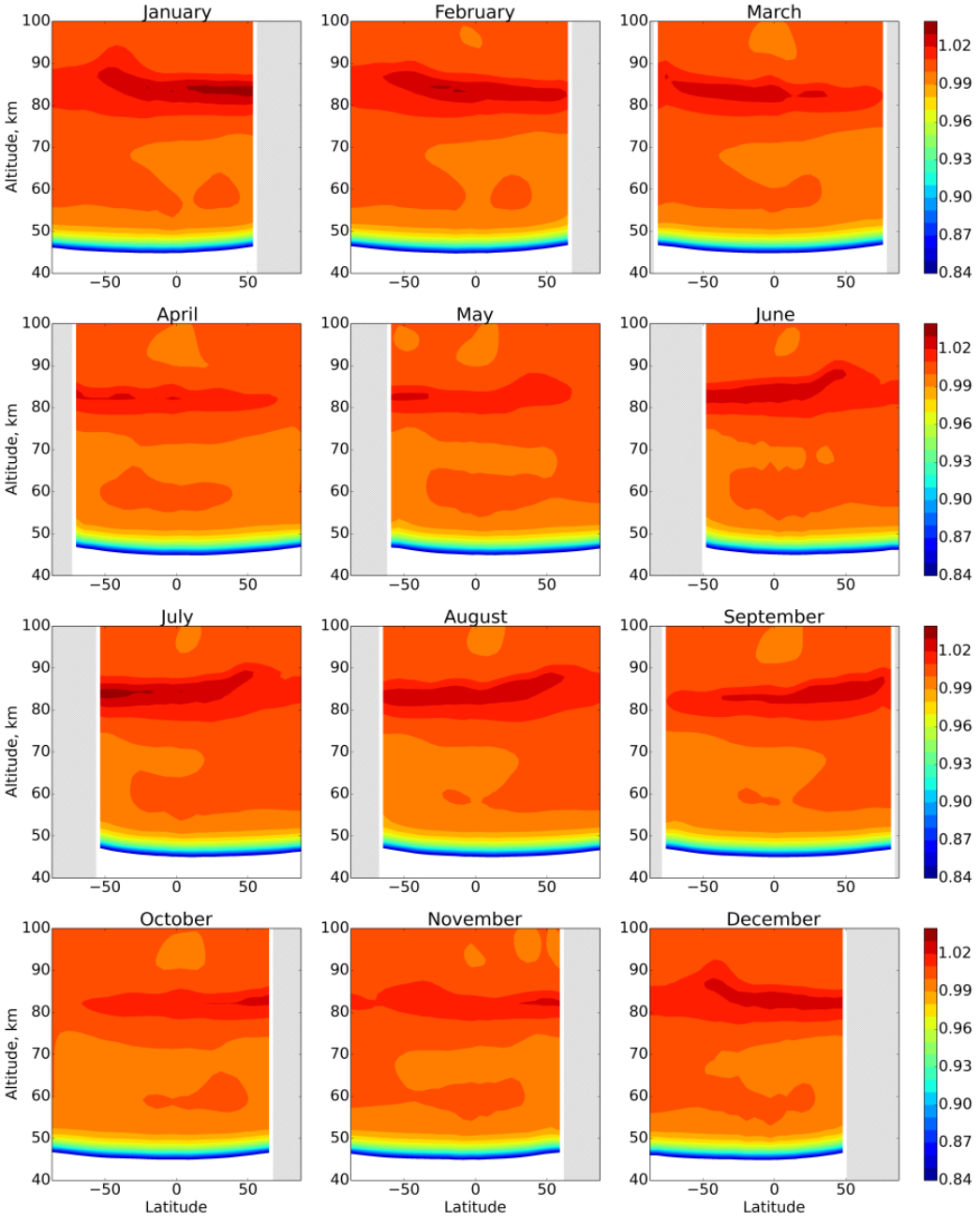

677

678

679 Figure 1. Daytime monthly averaged zonal mean $< F >$ distributions.

680

Atmos. Chem. Phys. Discuss., https://doi.org/10.5194/acp-2017-738
Manuscript under review for journal Atmos. Chem. Phys.
Discussion started: 10 November 2017

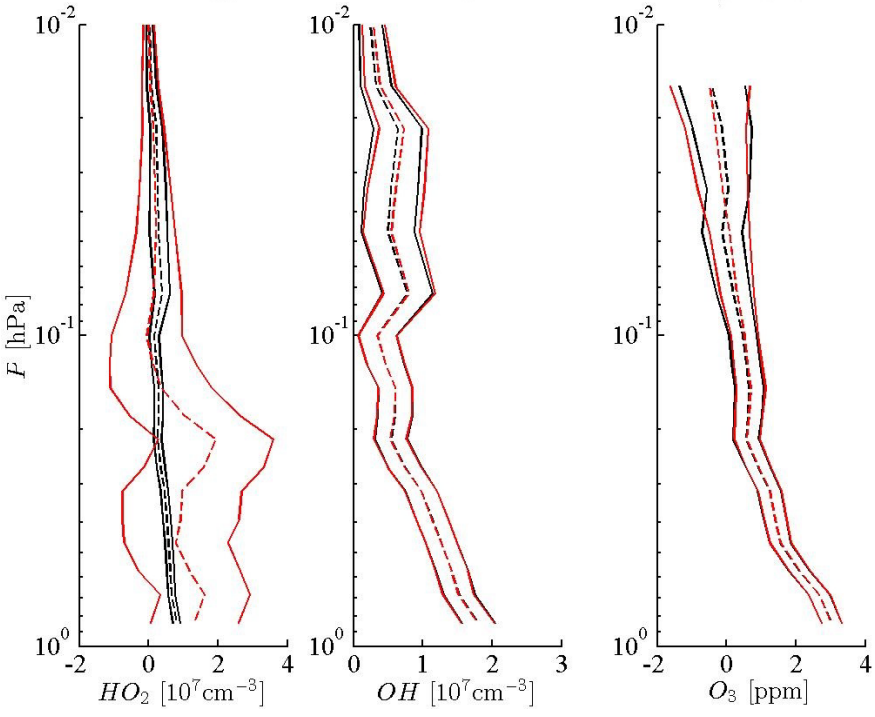

Figure 2. Example of OH, HO_2 and O_3 vertical profiles measured (red curves) on 15 January 2005 at 13.07 UT, 38.53^{0}N, 357.33^{0}W and corresponding retrieved profiles (black curves). Solid curves: boundaries of the 65% confident intervals, dashed curves: medians.

Atmos. Chem. Phys. Discuss., https://doi.org/10.5194/acp-2017-738
Manuscript under review for journal Atmos. Chem. Phys.
Discussion started: 10 November 2017

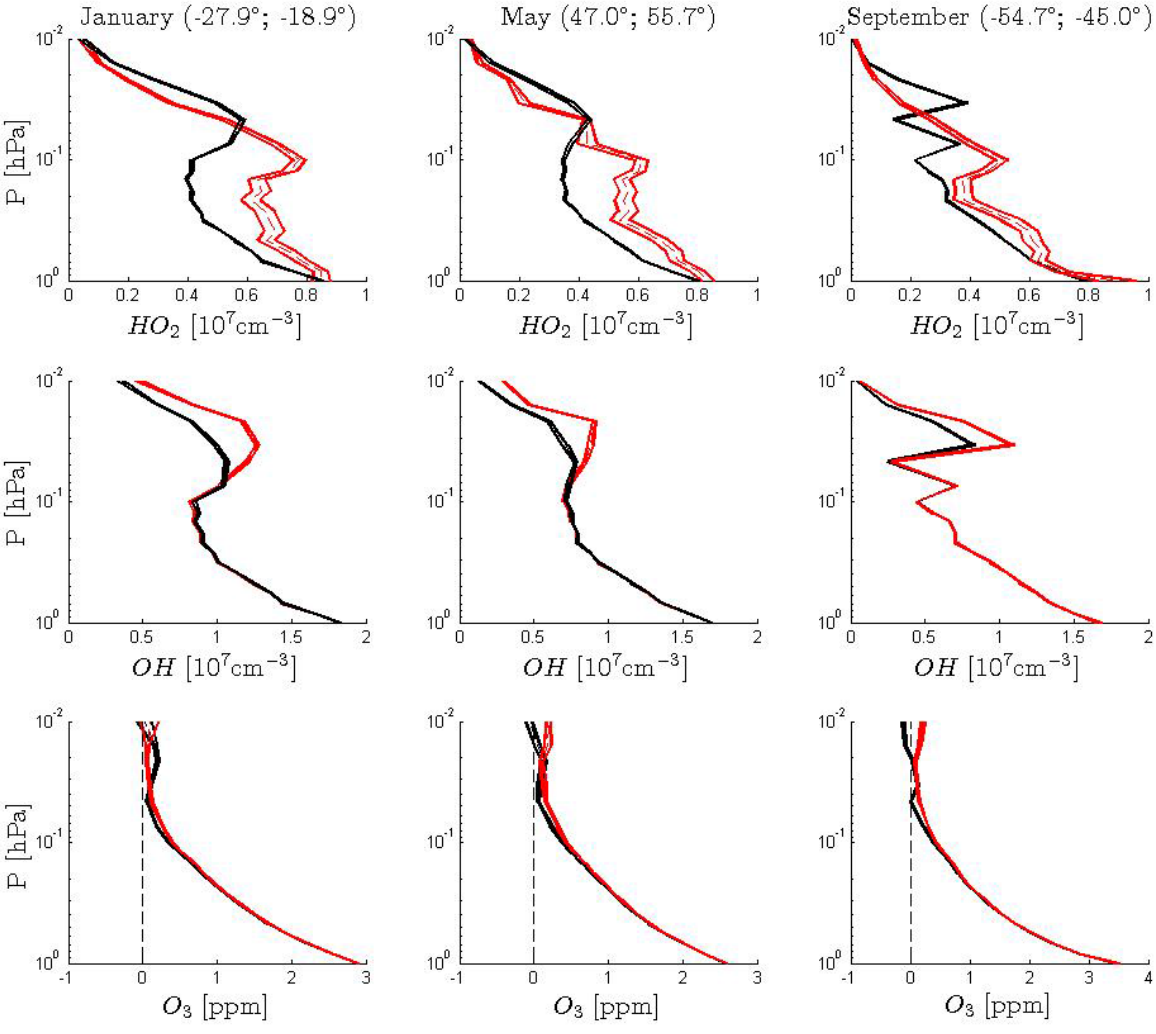

Figure 3. Examples of monthly averaged zonal mean vertical profiles of OH, HO_2 and O_3 measured (red curves) in January, May and March 2005 and corresponding retrieved profiles (black curves). Solid curves: boundaries of the 65% confident intervals, dashed curves: medians.

Atmos. Chem. Phys. Discuss., https://doi.org/10.5194/acp-2017-738
Manuscript under review for journal Atmos. Chem. Phys.
Discussion started: 10 November 2017

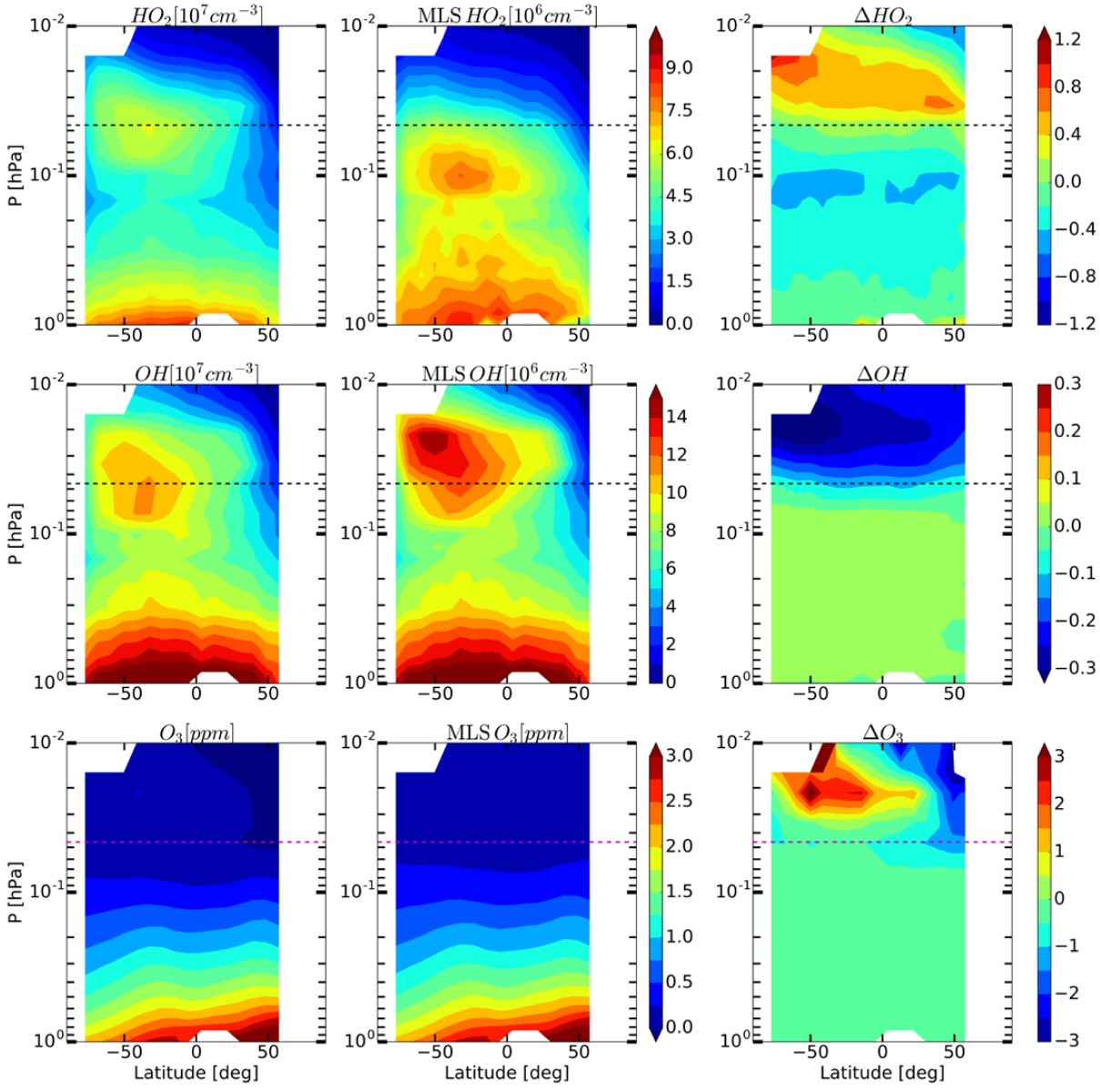

Figure 4. Daytime monthly averaged zonal mean retrieved (left column) and measured (middle column) distributions of HO_2, OH, and O_3 and their relative difference (right column) in January 2005.

Atmos. Chem. Phys. Discuss., https://doi.org/10.5194/acp-2017-738
Manuscript under review for journal Atmos. Chem. Phys.
Discussion started: 10 November 2017

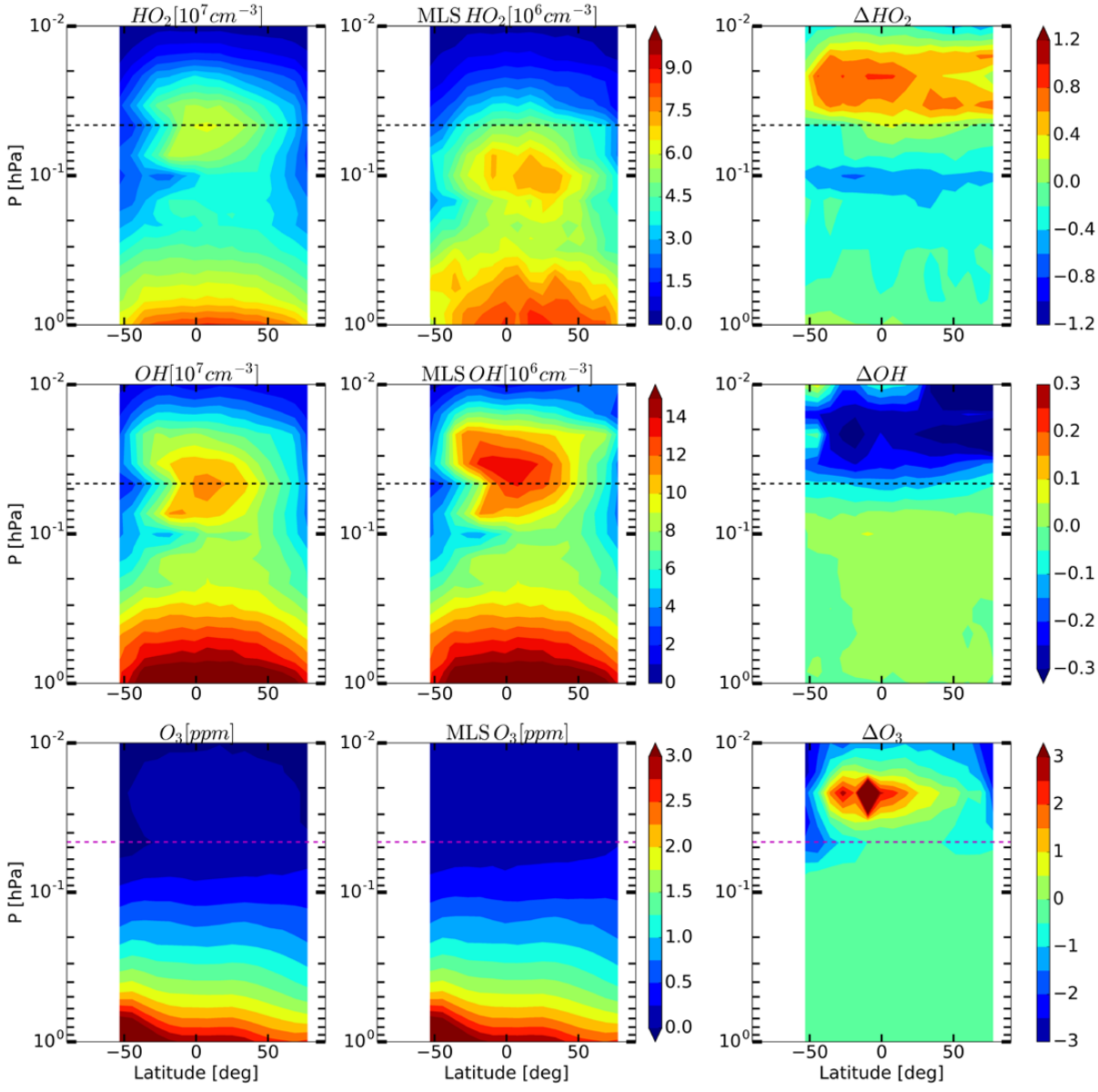

Figure 5. Daytime monthly averaged zonal mean retrieved (left column) and measured (middle column) distributions of HO_2, OH, and O_3 and their relative difference (right column) for May 2005.

Atmos. Chem. Phys. Discuss., https://doi.org/10.5194/acp-2017-738
Manuscript under review for journal Atmos. Chem. Phys.
Discussion started: 10 November 2017

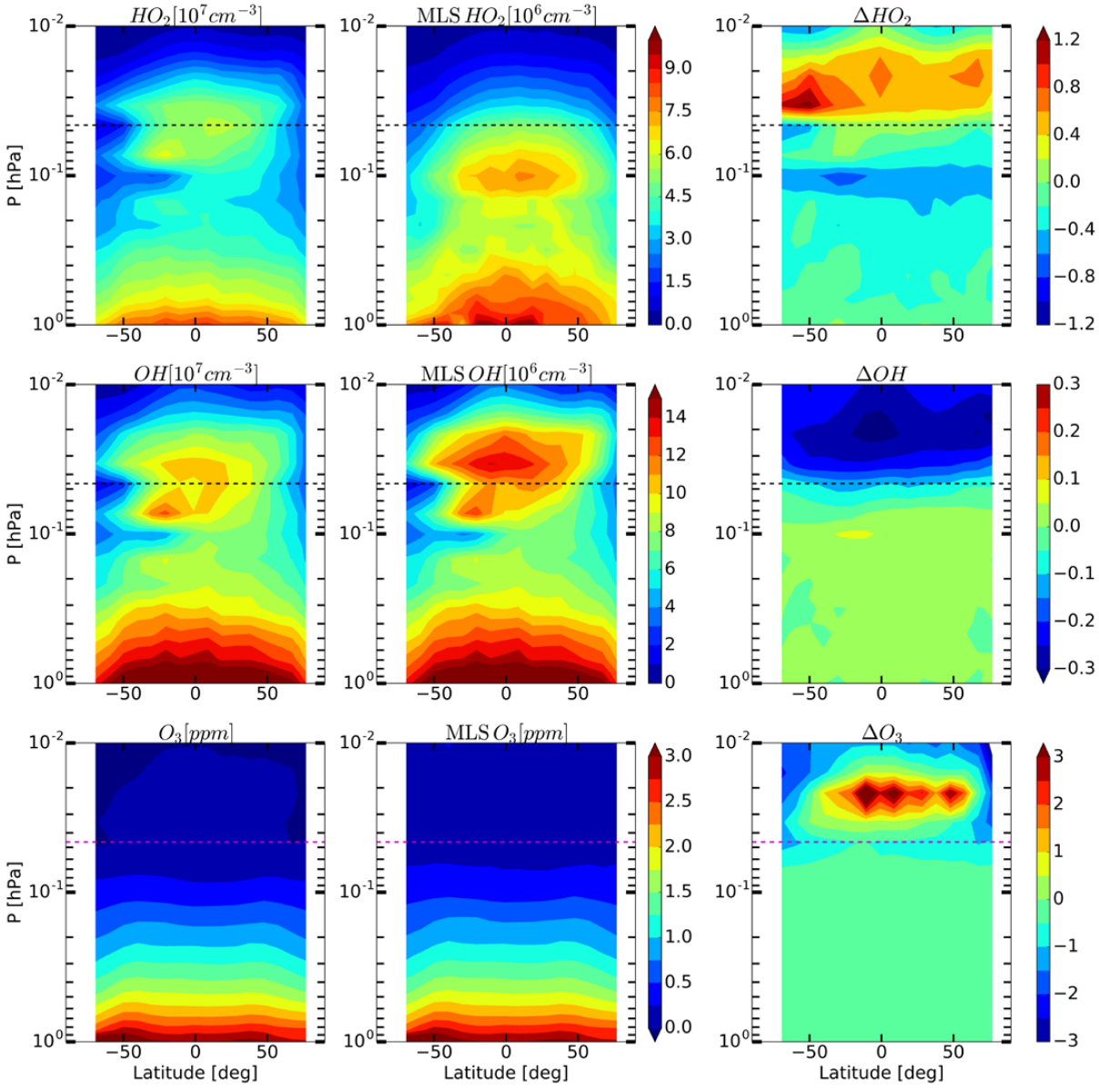

Figure 6. Daytime monthly averaged zonal mean retrieved (left column) and measured (middle column) distributions of HO_2, OH, and O_3 and their relative difference (right column) for September 2005.

Atmos. Chem. Phys. Discuss., https://doi.org/10.5194/acp-2017-738
Manuscript under review for journal Atmos. Chem. Phys.
Discussion started: 10 November 2017

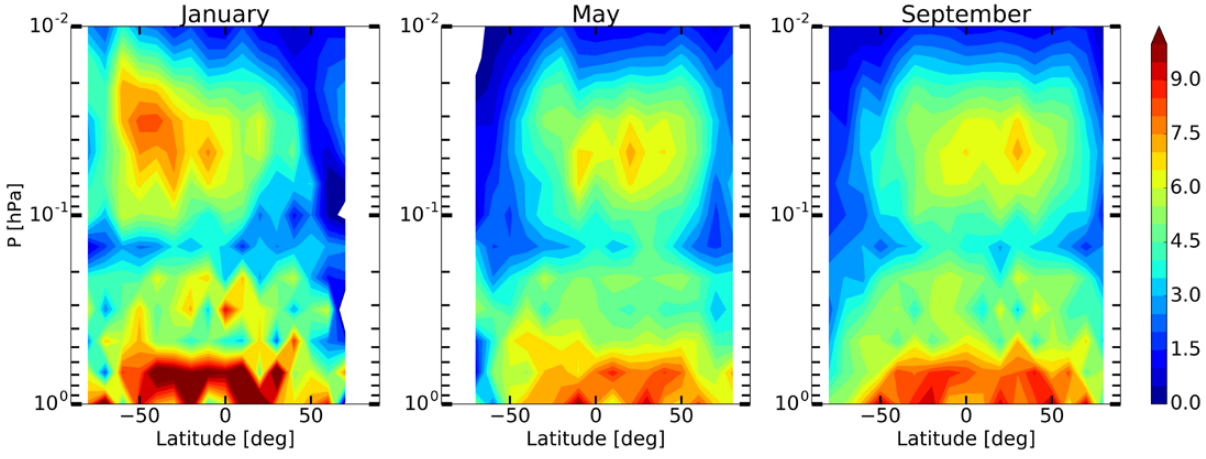

Figure 7. Daytime mean monthly averaged distributions of HO_2 retrieved by Millán et al. (2015) from MLS primary data.